Influence of the Electrical Double Layer in Electrowetting

Anthony Quinn, Rossen Sedev, and John Ralston*

Ian Wark Research Institute, University of South Australia, Mawson Lakes, SA 5095, Australia

Received: July 16, 2002

Electrowetting (wetting under the influence of an applied electric field) of three fluoropolymer surfaces (amorphous Teflon, DuPont) by electrolyte solutions was studied with the sessile drop method. The electrowetting curve (contact angle/potential) is analogous to the electrocapillary curve (surface tension/potential) and may be described by a combination of the Young and Lippmann equations. The influence of the electrical double layer at the polymer/solution interface has been neglected in the past because the overall interfacial capacitance is mainly determined by the capacitance of the insulating polymer layer. We demonstrate that for some surfaces a systematic deviation occurs at positive potentials. This departure from the constant capacitance regime is attributed to double layer effects, namely, the adsorption of hydroxide and halide anions. The pH, ionic strength, and polymer composition can all influence electrowetting behavior.

Introduction

The equilibrium contact angle, θ, at the three-phase contact line is given by the Young equation:

$$\gamma \cos \theta = \gamma_{SV} - \gamma_{SL} \quad (1)$$

where γ, γ_{SV}, and γ_{SL} are the interfacial tensions associated with the liquid/vapor, solid/vapor, and solid/liquid interfaces. If an external voltage is applied across the solid/liquid interface, the contact angle diminishes.

The most common experimental configuration consists of a drop of electrolyte solution resting on top of an electrode insulated with a thin (thickness *d* about a micrometer) polymer layer (Figure 1). The effect is referred to as electrowetting and has attracted significant interest in the past decade.[1]

The earliest reported use of the term electrowetting appears in a patent entitled "Electrowetting reproduction process",[2] which describes the use of an external electric potential (30−800 V) for improving the wettability of insulating hydrophobic surfaces with respect to ionically conductive liquids (typically from $\theta_0 = 120°-145°$ to $\theta = 45°-85°$).

The influence of electric charge on the interfacial tension of the mercury/aqueous solution interface is well-known and harks back to the classic work of Lippmann.[3] Electrocapillary measurements on solid electrodes have been pursued by many authors (e.g., refs 4 and 5 and references therein). Frumkin and co-workers recognized that a potential originating from an external source will influence the solid/liquid interface only (because the gas phase is a good insulator) and therefore changes in γ_{SL} can be followed by monitoring the contact angle. Experiments confirmed that $\gamma_{SL}(V)$ and $\theta(V)$ for the mercury electrode follow a similar trend and the electrocapillary maximum practically coincided with the electrowetting maximum.[6] On solid metals, only $\theta(V)$ measurements are feasible, but they turned out to be irreproducible and interest faded away (since then alternative methods have been devised[5]). Decades later, Morcos revived the approach by successfully employing the capillary rise method. He obtained consistent results for metals, semiconductors, and insulating electrodes.[4] Sondag-Huethorst and Fokkink carried out detailed studies of gold electrodes modified with thiol self-assembled monolayers.[7−9] The agreement between wettability and electrochemical measurements was good as long as the thiol layer was stable. The capacitance of the system was practically constant and determined mainly by the thickness and dielectric constant of the self-assembled layer.[8]

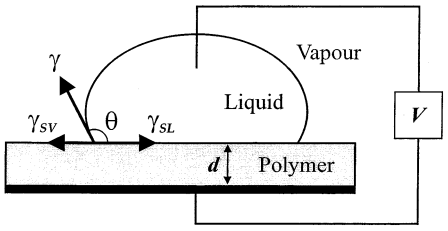

Figure 1. Sessile drop setup for electrowetting measurements.

Sparnaay[10] seems to be the first to use the arrangement depicted in Figure 1. He studied electrolyte droplets on the flat (111) surface of a Ge crystal. The contact angle decreased as the voltage was applied, but the values were scattered excessively. The earliest determination of contact angles on an insulating surface at different voltages is that of Chudleigh.[11] He reported angles (captive bubble technique) of water (at normal, acidic, and basic pH) and ethanol on Teflon FEP (fluorinated ethylene propylene) surfaces. At 1000 V negative voltage, all contact angles decreased by 10−20% from their initial values (the FEP samples were 25 μm thick).

Berge and co-workers[12,13] studied the electrowetting of poly(tetrafluoroethylene) (PTFE) and poly(ethylene terephthalate) (PET) by drops of aqueous NaCl. These systems, as distinct from earlier examples, permitted larger voltages (several hundred volts) to be applied while maintaining a negligible current flow. Therefore larger reversible changes of the contact angle (up to 70°) could be realized without inducing electrochemical reactions. Significant advances in the field followed rapidly with respect to instrumentation,[14] type of insulating coating,[15,16] electrowetting in solid/water/oil systems[17] and under dynamic conditions,[14,18−20] and theoretical interpretations.[21−23] This renewed interest was and is stimulated by the possible use of

* To whom correspondence should be addressed. Phone: +61 8 8302 3066. Fax: +61 8 8302 3683. E-mail: john.ralston@unisa.edu.au.

10.1021/jp0216326 CCC: $25.00
Published on Web 01/08/2003

electrowetting for applications such as liquid micromanipulation,[24−26] liquid movement in capillary arrays,[27] and the variation of the focal length of a liquid lens.[28]

Current electrowetting theory assumes that γ_{SL} is composed of two contributions[10,29]—chemical, γ_{SL}^0, and electrical (potential-dependent), γ_{SL}^V:

$$\gamma_{SL} = \gamma_{SL}^0 + \gamma_{SL}^V = \gamma_{SL}^0 - \frac{1}{2}CV^2 \qquad (2)$$

where V is the applied DC voltage. The quadratic term is obtained by integrating Lippmann's equation at constant C, capacitance per unit area of the insulating polymer layer. The latter can be modeled as a parallel-plate capacitor, and by combining eqs 1 and 2, we arrive at

$$\cos\theta = \cos\theta_0 + \frac{1}{2}\frac{\epsilon\epsilon_0}{\gamma d}V^2 \qquad (3)$$

where ϵ is the dielectric constant of the polymer and ϵ_0 is the permittivity of a vacuum.

It is largely accepted that eq 3 provides a good description of electrowetting data as long as the voltage does not exceed a certain critical limit. Beyond this threshold, the contact angle remains constant (unaffected by the increasing voltage). Different explanations have been proposed for this saturation effect,[21−23] but no definite agreement on the causes has yet been reached. Blake et al.[19] have argued that the correct numerical factor in eq 3 is $^1/_4$ rather than $^1/_2$, while Janocha et al.[17] have reported values between 0.5 and 0.01. The weight of experimental evidence points to 0.5, in agreement with eq 3.

Peculiar behavior at the three-phase contact line, as opposed to the whole solid area occupied by the drop, has been observed repeatedly (e.g., local polymer hydrophilization,[13] reduced coalescence between adjacent drops,[1] air ionization,[21] small droplet expulsion[13,21,30]). It has been suggested that the electrowetting effect is entirely due to line (rather than surface) tension effects;[31] however, this idea has gained little acceptance[1].

An electrical double layer is formed at the surface of a neutral polymer when it is immersed in water,[32] and therefore, the capacitance of the solid/liquid interface (Figure 1) consists of both polymer and double layer contributions.[8] The latter however, is usually much larger, and because the capacitors are in series, only the polymer contribution appears in eq 3; conventional opinion dictates that double layer effects are negligible. Indeed it has been reported that electrowetting is not affected by salt type or concentration.[12,14,22]

Deviations from the behavior prescribed by eq 3 for a range of solids have been noted; however, only rarely has it been speculated that a material deficiency may be the cause.[16] In this investigation, our focus is fixed firmly on how fluoropolymer composition and electrical double layer contributions can influence electrowetting. It is important to note that thin fluoropolymer films with excellent dielectric strength quality may be prepared in a straightforward fashion. We report results for three different grades of amorphous Teflon (Teflon AF). The study is limited to advancing angles and voltages below the saturation threshold. Deviations at positive potentials are found experimentally and attributed to double layer effects.

Materials and Methods

The insulating materials studied are amorphous fluoropolymers belonging to the Teflon AF line developed by DuPont.[33,34] Teflon AF is a random copolymer of 4,5-difluoro-2,2-bis-(trifluoromethyl)-1,3-dioxole (PDD) and tetrafluoroethylene (TFE), Figure 2.

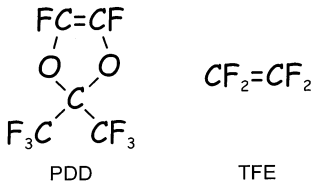

Figure 2. Structure of the two monomers of Teflon AF.

TABLE 1: Glass Transition Temperature, T_g, PDD Content, Dielectric Constant, ϵ, and Critical Surface Tension, γ_C, of the Teflon AF Variants Used in This Study

grade	T_g (°C)	PDD (mol %)	ϵ	γ_C[a] (mN/m)
T1	36[b]	<1[c]	2.1[d]	15.6
T2	133[b]	61[c]	2.1[d]	13.0
T3[e]	160[f]	65[f]	1.93[f]	12.7

[a] Values determined by linear extrapolation of cos θ versus liquid surface tension to $\theta = 0$ for four alkanes (C_6, C_7, C_8, and C_{16}). [b] Quoted by DuPont. [c] Estimated from the T_g versus TFE content relation.[33] [d] Value for PTFE.[34] [e] Trade name "Teflon AF1600" (DuPont). [f] Reference 34.

These fluoropolymers are soluble in fluorinated solvents and can be deposited as thin films by dip or spin coating techniques. The surface of these films is very hydrophobic (advancing contact angle of water at pH = 5.6 is 120° ± 2°) but also very smooth (rms roughness ≈ 0.4 nm and peak-to-valley height < 2 nm over 10 × 10 μm^2 [18]). The good quality of the surface is evidenced by the low (<10°[18]) contact angle hysteresis. Experiments have been conducted using three different Teflon AF variants: T1, T2, and T3, the properties of which are listed in Table 1 (variants T1 and T2 were made available by Dr. R. A. Hayes, Philips Research Laboratories; their spectroscopic and other properties have been described by Nason and Lu;[35] T3 (Teflon AF1600) was purchased directly from DuPont).

Teflon AF was dissolved in FC-75 fluorocarbon solvent (perfluoro-2-butyltetrahydrofuran, 3 M) and filtered through a 1 μm glass fiber filter to remove particulate contamination, and films were deposited onto gold-coated silicon wafers via dip coating. Coherent films without detectable pinholes or other defects were obtained (e.g., smooth surfaces were observed by AFM imaging). By varying the solution concentrations (1−6 wt %) and the speed of withdrawal (0.1−1 mm/s), we achieved final film thicknesses between 0.1 and 10 μm routinely. Polymer films were dried for 10 min in a laminar flow cabinet, followed by an additional 10 min drying at 110 °C to remove any residual solvent. Freshly prepared polymer films were used in all experiments.

All aqueous solutions were prepared with Milli-Q water (conductivity 5.6 μS/m; surface tension 72.8 mN/m) and analytical reagent grade salts. The normal pH of water was 5.6, and AR grade HCl and KOH were used to adjust the pH of the solutions when desired.

The experimental apparatus was based on the system developed by Verheijen and Prins,[14] in which the capacitance of a flat insulator-coated electrode contacted with a grounded droplet was measured as a function of the applied DC potential. The capacitance was then used to determine the solid/liquid interfacial area. For a known drop volume (e.g., 10 μL), the contact angle was obtained from the base area by a calibrated empirical equation. In addition, contact angles were independently determined from images of the sessile drop by numerically fitting a tangent close to the contact line. The data obtained by the two methods agreed to within 3%.

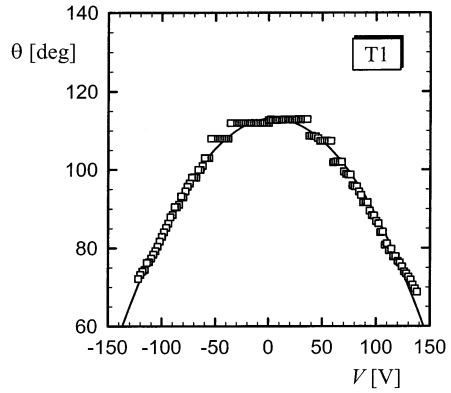

Figure 3. Electrowetting data (□) for 0.1 M KCl (pH = 5.6) on 2.0 μm thick T1 (T_g = 36 °C). The theoretical prediction (—) is calculated via eq 3.

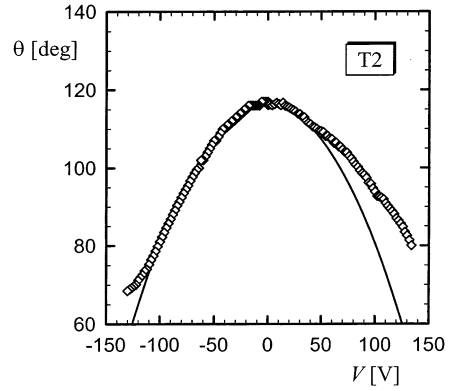

Figure 4. Electrowetting response (◇) of 0.1 M KCl (pH = 5.6) on 1.8 μm thick T2 (T_g = 133 °C). The theoretical prediction (—) is calculated via eq 3.

A microsyringe was used to very slightly advance the droplet at the beginning of each experiment to ensure that the contact angle was advancing prior to the actual voltage application. Small voltage increments (2 or 5 V) were used to resolve small contact angle deviations. Each experiment was conducted on a fresh area of surface to avoid effects associated with residual polymer charging.[22] Occasional data involving higher or unstable values of the dissipation factor, tan δ, were discarded from further consideration. Data with tan $\delta \geq 0.05$ normally arise as a result of poor polymer film preparation (e.g., the presence of contaminant particles results in leakage currents). Every curve was reproducibly repeated three to five times. Unless otherwise indicated, all experiments were conducted at 22 °C.

Results

A typical electrowetting curve for the T1 Teflon variant (lowest T_g) is plotted in Figure 3. The points represent the experimental results, while the solid line is calculated via eq 3. When the data were fitted, both θ_0 and the quadratic coefficient were treated as free parameters. The fitted estimates of the numerical factor were close to the theoretical value of $^1/_2$, having values ranging from 0.40 to 0.55. As shown in Figure 3, the theoretical behavior is obeyed very closely at both negative and positive potentials. A typical result for T2 is presented in Figure 4. In this case, the theoretical behavior is followed only at negative potentials, provided that the saturation limit (~120 V) is not exceeded. At positive potentials however, a marked deviation is seen above 50 V; the contact angle still decreases with external voltage but more gradually than predicted by eq 3. Results for T3 are quite similar (Figure 5).

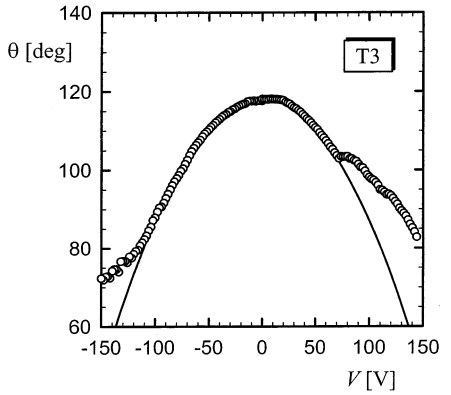

Figure 5. Electrowetting response (○) of 0.1 M KCl (pH = 5.6) on 2.4 μm thick T3 (AF1600; T_g = 160 °C). The theoretical prediction (—) is calculated via eq 3.

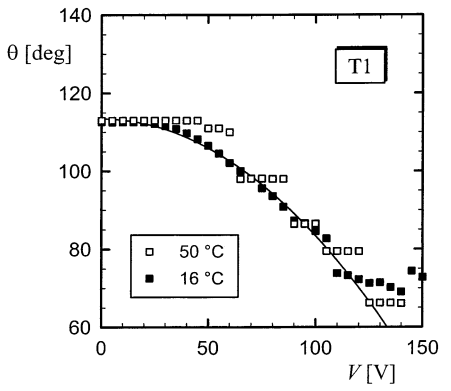

Figure 6. Electrowetting response for 0.1 M KCl (pH = 5.6) on 2.1 μm thick T1 (T_g = 36 °C) at 16 °C (■) and 50 °C (□). The theoretical prediction (—) is calculated via eq 3.

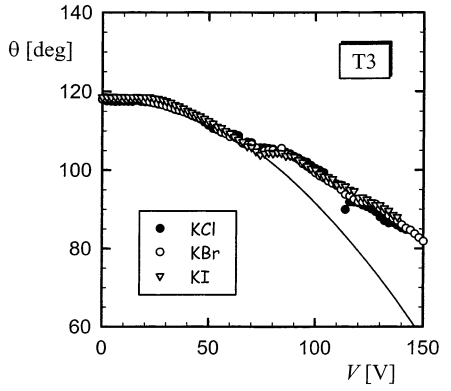

Figure 7. Electrowetting response for 0.1 M potassium salts (pH = 5.6) on 2.5 μm thick T3 (AF1600; T_g = 160 °C): KCl (●), KBr (○), and KI (▽). The theoretical prediction (—) is calculated via eq 3.

Because one major difference among the three copolymers appears to be the glass transition temperature (Table 1), electrowetting studies on T1 were conducted at temperatures above and below its T_g, the results of which are shown in Figure 6. Apart from somewhat more sporadic wetting behavior at the elevated temperature (50 °C), the two results are in very good agreement and again follow closely the parabolic decrease described by eq 3.

Because the bulk properties of the Teflon variants are quite similar, the possible influence of the polymer/solution interface was further explored. The substitution of KBr or KI for KCl had no detectable effect on the electrowetting curve (Figure 7). However, ionic strength turned out to be an important factor.

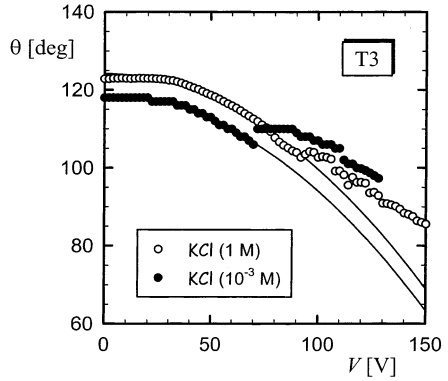

Figure 8. Electrowetting response for 1.0 M KCl (○) and 10^{-3} M KCl (●) at pH = 5.6 on 2.2 μm thick T3 (AF1600; T_g = 160 °C). The theoretical predictions (—) are calculated via eq 3.

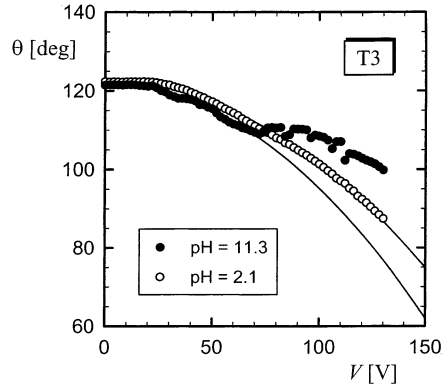

Figure 9. Electrowetting response for 0.1 M KCl on 2.2 μm thick T3 (AF1600; T_g = 160 °C) at pH = 2.1 (○) and pH = 11.3 (●). The theoretical predictions (—) are calculated via eq 3.

As can be seen in Figure 8, at increased salt concentration the theoretical prediction is valid over a wider voltage range.

Figure 9 shows the strong dependence of electrowetting on the pH of the liquid at positive voltages. At the lowest value (pH = 2.1), the correlation with theory is satisfactory up to the saturation limit (~130 V). As the pH is changed through neutral to basic, the deviation from eq 3 becomes progressively more pronounced. At pH = 11.3, deviation from theory is already apparent at approximately 70 V.

Discussion

Electrowetting has been carried out previously on PTFE[12,13,20] and Teflon AF1600[16] surfaces. The agreement between experiment and theory, below the saturation limit, was reportedly quite good. We confirm this for the T1 variant only (Figures 3 and 6). As the PDD content increases, deviations from theory at positive voltages become significant (Figures 4 and 5).

The departure from the ideal electrowetting behavior described by eq 3 seems hardly attributable to different bulk properties. The only bulk material parameter related to the polymer that explicitly enters into eq 3 is the dielectric constant, ϵ. The values for the three Teflon variants are very similar (Table 1), yet even if they were not, they could not account for the type of deviation observed in our experiments (Figures 4 and 5). Because the best agreement between theory and experiment was observed for T1, the Teflon with the lowest T_g, it was hypothesized that chain mobility might be of some importance. The T1 fluoropolymer is indeed softer than T2 and T3, as was qualitatively confirmed by AFM imaging in tapping mode. Experiments performed above and below the T_g conclusively show (Figure 6) that compliance with eq 3 is not affected by temperature changes. Interestingly, electrowetting at elevated temperature is more sporadic. It thus appears that when chain mobility is higher, the stress present at the contact line is strong enough to affect the polymer surface locally and this translates into a pronounced pinning of the contact line.

Because the bulk properties of the three polymers are quite similar, it was concluded that the difference between them was interfacial in nature. It is well documented that neutral polymer surfaces in aqueous electrolyte solutions exhibit negative ζ potentials.[32] The negative charge at the polymer/solution interface is most often attributed to specific adsorption of anions (usually Cl^- and OH^-). The latter are more polarizable and less hydrated, and this promotes their tendency to partition at the interface.[32] The phenomenon is also commonly observed at the water/air and water/oil interfaces.[36−38] Recently, Zimmerman et al.[39] have reported electrokinetic and surface conductivity measurements on Teflon AF1600 surfaces. A negative charge was found and ascribed to the preferential adsorption of hydroxide ions. Thus the existence of a negative charge at the amorphous fluoropolymer/solution interface in the absence of an externally applied voltage is firmly established.

As already indicated, the electrowetting curve is essentially analogous to the electrocapillary curve. This analogy is further stressed by several observations: (i) deviations occur at positive potentials only (Figures 4 and 5); (ii) halide anions have no appreciable effect (Figure 7); (iii) ionic strength is a significant factor (Figure 8); (iv) pH of the solution is of paramount importance (Figure 9). All of these facts imply that the electrical double layer at the polymer/solution interface is the root cause of this nonideal electrowetting behavior.

The scale of the deviation can be estimated as follows. The contact angle decrease is shallower than predicted, that is, to reach a contact angle predicted by eq 3, an excess positive voltage, V^*, is required. Under these conditions, eq 3 becomes

$$\theta = \theta_0 - \frac{C}{2\gamma}(V - V^*)^2 \tag{4}$$

where V is the actual applied voltage and $V - V^*$ represents the corrected or ideal voltage at the solid/liquid interface. This voltage shift is (e.g., see Figure 5) $V^* \approx 35$ V at $V = 140$ V. It represents an energy loss during charging. The charge density, σ^*, due to adsorbed charges is

$$\sigma^* = \frac{\epsilon\epsilon_0}{d}V^* \approx 2.5 \times 10^{-4}\ \text{C/m} \tag{5}$$

The magnitude of this charge is rather small particularly when compared with a metal oxide/water interface.[40] van Wagenen et al.[41] have performed extensive streaming potential measurements for several neutral polymer surfaces (including polystyrene, poly(vinyl chloride), and polydimethyl siloxane) and quoted a typical surface charge density of 4.8×10^{-3} C/m^2. Using a very different technique (electrons injected in thin polymer layers), Fowkes and Hielscher[42] obtained a limiting surface charge density for polystyrene and chlorinated polyethylene of about $1.6-1.8 \times 10^{-3}$ C/m^2. Zimmerman et al.[39] calculated a charge density of 5×10^{-3} C/m^2 for Teflon AF1600 in 1 mM KCl. Therefore, the magnitude of the deviations reported here can be attributed with some confidence to the effect of the double layer existing at the polymer/solution interface.

It should be noted that eq 4 is formally identical to the one proposed by Verheijen and Prins[22] to explain contact angle

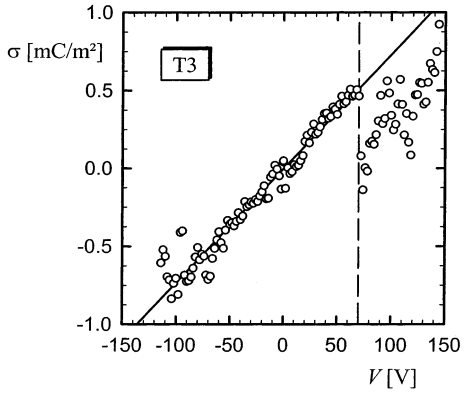

Figure 10. Surface charge density on the electrode, σ, as a function of the applied voltage, V (data from Figure 5). The slope of the solid line gives the same capacitance per unit area (7.3 μF/m) as that shown in Figure 5.

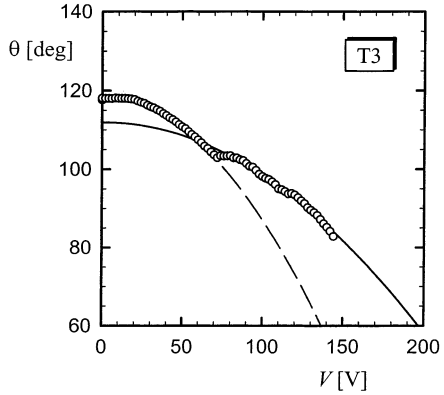

Figure 11. Positive potential branch of the electrowetting curve shown in Figure 5. The solid line is given by eq 3 (the dashed line is taken from Figure 5).

saturation. In their model, beyond a certain threshold voltage (positive or negative), charge trapping occurs "in or on" the polymer layer beyond the three-phase contact line, that is, on the "dry" polymer surface. Supposedly, this counteracts exactly the electrowetting effect and hence leads to saturation. Our discussion is restricted to deviations that take place below the saturation limit. Moreover, the deviations that we report are asymmetric with respect to polarization, ion specific, and concentration-dependent, in contrast to the picture presented in ref 22. Therefore, the above similarity (a diminished electrowetting effect) is only apparent because the effects that we observe arise from adsorption phenomena at the fluoropolymer/aqueous solution interface.

It is possible to obtain the surface charge density from the electrocapillary curve in much the same way as from electrocapillary curves. The charge density on the electrode, σ, is given by the Lippmann equation:[3,7]

$$\sigma = -\frac{\partial \gamma_{SL}}{\partial V} = -\gamma \frac{\partial \theta}{\partial V} \tag{6}$$

where use of eq 3 was made. The data from Figure 5 were numerically differentiated, and the resulting charge density is presented as function of the applied voltage in Figure 10. From -100 to 70 V, σ increases linearly and the slope gives the same value for the capacitance per unit area as the fit shown in Figure 5 (7.1 μF/m). At positive polarization beyond this range, charging becomes less effective. In view of the larger scatter, the data are approximated with a linear trend, that is, constant capacitance. This provides a fair description of the deviation, as is seen in Figure 11. Here, only the positive potential branch of Figure 5 is presented. The curvature of the solid parabola passing through the deviation is about half that of the dashed one. In this regime, the "effective" contact angle at zero external voltage is significantly lower (112° versus 118°).

Specific ion adsorption most certainly occurs at solid/aqueous solution and Hg/aqueous solution interfaces.[3,6,40,43] With this knowledge and the recent picture of specific hydroxide ion adsorption at the water/air interface presented by Karraker and Radke,[38] the following qualitative physical model can be outlined. Some OH^- ions are specifically adsorbed at the polymer surface even in the absence of any external voltage. Most probably, they are partially dehydrated.[38] When positive voltage is applied, the insulator is polarized and attracts anions from the solution, that is, more ions adsorb.[43] Adsorption of OH^- saturates at a certain voltage,[38] and further ion adsorption is obstructed. Thus charging efficiency is reduced, and deviations in the electrowetting curve are observed at positive potentials (at negative potentials, OH^- are electrostatically repelled and no such complications arise).

This picture is consistent with our observations. Anions, which are not specifically adsorbed (Cl^-, Br^-, I^-), do not affect the process (Figure 7). The situation strongly depends on the pH of the solution (Figure 9); a higher OH^- concentration reduces the contact angle (although marginally) even without external voltage. Charging at high pH, that is, at high OH^- concentration, is impeded already at 70 V, while at low pH, the contact angle decrease follows eq 3 up to 130 V. At normal pH (Figure 11), the deviation occurs at about the same voltage ($\sim$70 V) and the value of the contact angle extrapolated to zero external voltage is reduced (reflecting the limiting OH^- adsorption). Ionic strength increases θ_0 (Figure 8), even though the liquid surface tension increases by about 2%.[44] This effect may be due to double layer compression[39] or partial OH^- desorption or both. Charging at higher ionic strength follows the theoretical trend up to 90 V (as compared to 70 V at lower ionic strength) and then becomes less effective. Additional experiments carried out in the presence of 1 M urea (a well-known water structure breaker[45]) yielded exactly the same results. Therefore water structure, per se, does not seem to be a factor.

Finally, we remark on the difference between the different Teflon grades. The T1 variant contains a minimal amount of PDD (which is apparently sufficient to disrupt the crystalline structure of TFE), and its electrowetting response conforms to eq 3. On the other hand, variants T2 and T3 contain significant amounts of PDD, and deviations at positive polarization are always found. Therefore, the magnitude of the deviation appears to be related to the amount of dioxole. It may be speculated that hydroxide ions have higher affinity toward the oxygen-containing monomers. Such hypothesis is partially supported by the larger ζ potential at basic pH measured for Teflon AF1600 in comparison to PTFE (e.g., -90 mV at pH = 9 in 10^{-3} M KCl[39] versus -40 mV for PTFE[46] under the same conditions).

The increasing amount of oxygen in the surface layer is convincingly, even though qualitatively, proven by time-of-flight secondary ion mass spectrometry (ToF$-$SIMS) measurements (Figure 12). However, the dependence of the critical surface tension on the PDD content reveals a somewhat different picture (Figure 13). The critical surface tension linearly decreases with the amount of dioxole, and all values fall within the range of wettability of PTFE (18.5 mN/m[48]) and closely packed perfluoromethyl groups (6 mN/m[48]). Thus, PDD is more hydrophobic than the TFE, which implies that its two $-CF_3$ groups

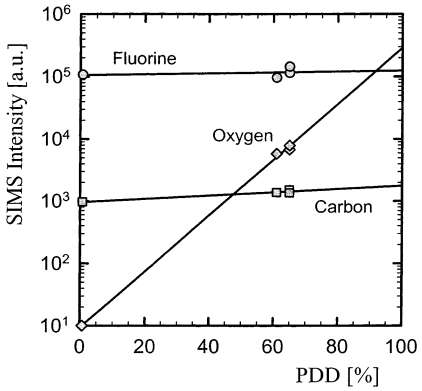

Figure 12. ToF−SIMS signal (negative mode) for the three Tefon AF variants.

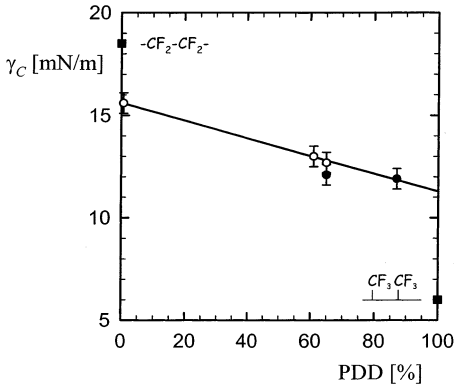

Figure 13. Critical surface tensions obtained from Zisman plots of the contact angles of several alkanes (○, this study; ●, ref 47) and tabulated values (■) for PTFE and closely packed prefluoromethyl groups.[48]

point outward[48] and quite effectively shield the dioxole ring. Thus, the role of the oxygen heteroatom in the surface layer is rather complex.

The dioxole monomer is responsible for the amorphous structure and the limited solubility of the Teflon AF copolymers in fluorinated solvents,[33,34] which are highly desirable qualities in technical applications. Larger electrowetting response at positive potential and better adherence to theory is found when the dioxole content is lower. Lower PDD content, however, decreases the T_g of the copolymer[33] and eventually the electrowetting curve becomes less smooth (cf. Figures 3, 4, and 5). These opposite tendencies must be considered in the specific context of any given application.

Conclusion

A diminished electrowetting response is observed at positive voltages on amorphous Teflon that contains larger amounts of dioxole monomer. The effect occurs before saturation of the contact angle and may be attributed to specific hydroxide ion adsorption. The marked influence of pH and ionic strength supports this hypothesis. These findings emphasize the analogy between electrowetting and electrocapillarity.

Acknowledgment. Financial support for this project from the Australian Research Council Special Research Centre Scheme and Philips Research Laboratories under Research Agreement RWC-061-PS-99044-ps is gratefully acknowledged. The authors are extremely grateful to Dr. R. A. Hayes (Philips Research Laboratories) for many in-depth discussions and for encouraging our research into amorphous fluoropolymers for use as dielectric materials for electrowetting.

References and Notes

(1) Quilliet, C.; Berge, B. *Curr. Opin. Colloid Interface Sci.* **2001**, *6*, 34.

(2) Minnesota Mining and Manufg. Co. GB Patent No. 1,087,431, 1967.

(3) Bockris, J. O'M.; Reddy, A. K. N. *Modern Electrochemistry*; Plenum Press: New York, 1970; Vol. 2, Chapter 7.

(4) Morcos, I. *J. Electroanal. Chem. Interfacial Electrochem.* **1975**, *62*, 313.

(5) Butt, H.-J.; Raiteri, R. In *Surface Characterization Methods*; Milling, A. J., Ed.; Marcel Dekker: New York, 1999; Chapter 1.

(6) Damaskin, B. B.; Petrii, O. A. *Introduction to Electrochemical Kinetics*, 2nd ed.; Vyshaya Shkola: Moscow, 1983; p 46 [in Russian].

(7) Sondag-Huethorst, J. A. M.; Fokkink, L. G. J. *Langmuir* **1992**, *8*, 2560.

(8) Sondag-Huethorst, J. A. M.; Fokkink, L. G. J. *J. Electroanal. Chem.* **1994**, *367*, 49.

(9) Sondag-Huethorst, J. A. M.; Fokkink, L. G. J. *Langmuir* **1995**, *11*, 2237.

(10) Sparnaay, M. J. *Surf. Sci.* **1964**, *1*, 213.

(11) Chudleigh, P. W. *J. Appl. Phys.* **1976**, *47*, 4475.

(12) Berge, B. *C. R. Acad. Sci. Paris* **1993**, *317-II*, 157.

(13) Vallet, M.; Berge, B.; Vovelle, L. *Polymer* **1996**, *37*, 2465.

(14) Verheijen, H. J. J.; Prins, M. W. J. *Rev. Sci. Instrum.* **1999**, *70*, 3668.

(15) Welters, W. J. J.; Fokkink, L. G. J. *Langmuir* **1998**, *14*, 1535.

(16) Seyrat, E.; Hayes, R. A. *J. Appl. Phys.* **2001**, *90*, 1383.

(17) Janocha, B.; Bauser, H.; Oehr, C.; Brunner, H.; Göpel, W. *Langmuir* **2000**, *16*, 3349.

(18) Schneemilch, M.; Welters, W. J. J.; Hayes, R. A.; Ralston, J. *Langmuir* **2000**, *16*, 2924.

(19) Blake, T. D.; Clarke, A.; Stattersfield, E. H. *Langmuir* **2000**, *16*, 2928.

(20) Decamps, C.; de Coninck, J. *Langmuir* **2000**, *16*, 10150.

(21) Vallet, M.; Vallade, M.; Berge, B. *Eur. Phys. J. B* **1999**, *11*, 583.

(22) Verheijen, H. J. J.; Prins, M. W. J. *Langmuir* **1999**, *15*, 6616.

(23) Peykov, V.; Quinn, A.; Ralston, *J. Colloid Polym. Sci.* **2000**, *278*, 789.

(24) Colgate, E.; Matsumoto, H. *J. Vac. Sci. Technol. A* **1990**, *8*, 3625.

(25) Washizu, M. *IEEE Trans. Ind. Appl.* **1998**, *34*, 732.

(26) Pollack, M. G.; Fair, R. B.; Shenderov, A. D. *Appl. Phys. Lett.* **2000**, *77*, 1725.

(27) Prins, M. W. J.; Welters, W. J. J.; Weekamp, J. W. *Science* **2001**, *291*, 277.

(28) Berge, B.; Peseux, J. *Eur. Phys. J. E* **2000**, *3*, 159.

(29) Fokkink, L. G. J.; Ralston, J. *Colloids Surf.* **1989**, *36*, 69.

(30) Mugele, F.; Herminghaus, S. *Appl. Phys. Lett.* **2002**, *81*, 2303.

(31) Digilov, R. *Langmuir* **2000**, *16*, 6719.

(32) Garbassi, F.; Morra, M.; Occhiello, E. *Polymer Surfaces*; John Wiley & Sons: Chichester, U.K., 1994; p 211.

(33) Hung, M.-H.; Resnick, P. R.; Smart, B. E.; Buck, W. H. In *Polymeric Materials Encyclopedia*; Salamone, J. C.; CRC Press: Boca Raton, FL, 1996; Vol. 4, p 2466.

(34) Brandrup, J., Immergut, E. H., Grulke, E. A., Eds. *Polymer Handbook*, 4th ed.; John Wiley & Sons: New York, 1999; p V/52.

(35) Nason, T. C.; Lu, T.-M. *Thin Solid Films* **1994**, *239*, 27.

(36) Kelsall, G. H.; Tang, S.; Yurdakul, S.; Smith, A. L. *J. Chem. Soc., Faraday Trans.* **1996**, *92*, 3887.

(37) Exerowa, D.; Kruglyakov, P. M. *Foam and Foam Films*; Elsevier: Amsterdam, 1998.

(38) Karraker, K. A.; Radke, C. J. *Adv. Colloid Interface Sci.* **2002**, *96*, 231.

(39) Zimmermann, R.; Dukhin, S.; Werner, C. *J. Phys. Chem. B* **2001**, *105*, 8544.

(40) Hunter, R. J. *Zeta Potential in Colloid Science*; Academic Press: London, 1981.

(41) van Wagenen, R. A.; Coleman, D. L.; King, R. N.; Triolo, P.; Brostrom, L.; Smith, L. M.; Gregonis, D. E.; Andrade, J. D. *J Colloid Interface Sci.* **1981**, *84*, 155.

(42) Fowkes, F. M.; Hielscher, F. H. *Org. Coat. Plast. Chem.* **1980**, *42*, 169.

(43) Habib, M. A.; Bockris, J. O'M. In *Comprehensive Treatise of Electrochemistry*; Bockris, J. O'M., Conway, B. E., Yeager, E., Eds.; Plenum Press: New York, 1980; Vol. 1, Chapter 4.

(44) Lide, D. R., Ed. *CRC Handbook of Chemistry and Physics*, 72nd ed.; CRC Press: Boca Raton, FL, 1991.

(45) Franks, F.; Reid, D. S. In *Water − A Comprehesive Treatise*; Franks, F., Ed.; Plenum Press: New York, 1973; Vol. 2, Chapter 5.

(46) Werner, C.; König, U.; Augsburg, A.; Arnhold, C.; Körber, H.; Zimmermann, R.; Jacobasch, H.-J. *Colloids Surf. A* **1999**, *159*, 519.

(47) Drummond, C. J.; Georgaklis, G.; Chan, D. Y. C. *Langmuir* **1996**, *12*, 2617.

(48) Zisman, W. A. In *Contact Angle, Wettability, and Adhesion*; Gould, R. F., Ed.; American Chemical Society: Washington, DC, 1964; Chapter 1.